2.1 Introduction

The current chapter discusses the detailed description of materials and experimental methodologies for the green synthesis of AgNPs and AuNPs and their nanocomposites which have been used for various applications. This chapter also deals with an overview of the various modern characterization techniques such as UV-visible spectroscopy, Fourier Transform-Infrared (FT-IR) Spectroscopy, Scanning Electron Microscopy (SEM), Transmission Electron Microscopy (TEM), Energy-Dispersive X-Ray Spectroscopy (EDS), Selected Area Diffraction Pattern (SAED Pattern), X-Ray Diffraction (XRD), Atomic Force Microscopy (AFM), X-Ray Photoelectron Spectroscopy (XPS), and Raman Spectroscopy. The experimental details of the preparation of leaf extracts, confirmation and quantification of polyphenolic compounds, green synthesis of AgNPs and AuNPs, and their optimization studies are discussed in this chapter. In addition to this, the synthesis of graphene oxide (GO), reduced graphene oxide (rGO), AgNPs-rGO-PANI, AuNPs-rGO nanocomposites are also covered in this chapter. In addition to this, the details procedures of various applications of AgNPs and AuNPs performed in the current study like antibacterial activity, antileishmanial activity, antioxidant activity, detection of iron (III), hydrogen peroxide (H_2O_2), glutathione and cholesterol are also discussed in this chapter.

2.2 Materials

The current study is based on the development of completely eco-friendly, economically viable and energy efficient route for the synthesis of AgNPs and AuNPs. The synthesis process was completely free from the chemicals, only the metal salts of silver and gold were the known chemicals used in the synthesis experiment of AgNPs and AuNPs. All the chemicals were used in the application part of this study which were of AR grade and

used without further purification. The name of the all the chemicals are listed in the **Table 2.1**. In the current work, Ultra pure water (UPW) prepared from Thermo Scientific Barnstead Smart2Pure Ultra Pure water system was utilized throughout the experiments. The pH and conductivity of the UPW were 7 and 0.055 μS/cm. The resistance was 18.2 MΩxcm at 25°C whereas the TOC was in the range of 5-10 ppb.

Table 2.1 List of chemicals

S. No.	Name	Chemical formula	Physical state	Manufacturer
1	Silver Nitrate	$AgNO_3$	Solid	Merck
2	Gold (III) Chloride hydrate	$HAuCl_4.xH_2O$	Solid	Sigma Aldrich
3	Ferric Chloride	$FeCl_3$	Solid	Sigma Aldrich
4	Iron (II) Chloride Tetrahydrate	$Cl_2Fe.4H_2O$	Solid	Alfa Aesar
5	Lead Nitrate	$Pb(NO_3)_2$	Solid	SD Fine-Chem Ltd.
6	Cadmium Nitrate	$Cd(NO_3)_2.4H2O$	Solid	SD Fine-Chem Ltd.
7	Cobaltous Nitrate	$Co(NO_3)_2.6H_2O$	Solid	SD Fine-Chem Ltd.
8	Zinc Sulphate	$ZnSO_4.7H_2O$	Solid	SD Fine-Chem Ltd.
9	Nickel Chloride	$NiCl_2.6H_2O$	Solid	Qualigens Fine-Chem Ltd.
10	Aluminium Nitrate	$Al(NO_3)_3.9H_2O$	Solid	Central Drug House Pvt. Ltd.
11	Arsenic tri-oxide	As_2O_3	Solid	SD Fine-Chem Ltd.
	Potassium dichromate	$K_2Cr_2O_7$	Solid	Alfa Aesar
12	Cupric Chloride	$CuCl_2.2H_2O$	Solid	SD Fine-Chem Ltd.
13	Mercuric Nitrate	$Hg(NO_3)_2.H_2O$	Solid	Loba-Chem
14	Manganous Chloride	$MnCl_2.4H_2O$		SD Fine-Chem Ltd.
15	Nutrient Agar (NA)	*****	Solid	Hi-Media
16	M199	*****		Hi-Media
17	Luria Bertani Broth	*****	Solid	Hi-Media
18	Mueller Hinton Agar (MHA)	*****	Solid	Hi-Media
19	Glutaraldehyde	$C_5H_8O_2$	Liquid	Sigma Aldrich
20	Ethanol	C_5H_5OH	Liquid	Sigma Aldrich
21	Hydrogen Peroxide	H_2O_2	Liquid	Merck
22	Methanol	CH_3OH	Liquid	Merck
23	Ascorbic Acid	$C_6H_8O_6$	Solid	Merck
24	1,1-Diphenyl-2-picrylhydrazyl (DPPH)	$C_{18}H_{12}N_5O_6$	Solid	Merck
25	Graphite powder (mess size 150 μm)	*****	Solid	Sigma Aldrich
26	Sulfuric acid	H_2SO_4	Liquid	Sigma Aldrich
27	Phosphoric acid	H_3PO_4	Liquid	Sigma Aldrich
28	Potassium permanganate	$KMnO_4$	Solid	Sigma Aldrich

29	Sodium hydroxide	NaOH	Solid	SD Fine-Chem Ltd
30	Nitric Acid	HNO_3	Liquid	SD Fine-Chem Ltd
31	Hydrogen peroxide	H_2O_2	Liquid	SD Fine-Chem Ltd
32	Hydrochloric acid	HCl	Liquid	SD Fine-Chem Ltd
33	Ammonium persulphate (APS)	$(NH_4)_2S_2O_8$	Solid	SD Fine-Chem Ltd
34	Hydrazine	NH_2NH_2	Solid	SD Fine-Chem Ltd
35	Ammonium hydroxide	NH_4OH	Liquid	SD Fine-Chem Ltd
36	Sodium Phosphate	Na_2HPO_4	Solid	Merck
37	Potassium Chloride	KCl	Liquid	Merck
38	Acetone	C_3H_6O	Liquid	Merck
39	Nafion solution	*****	Semi-liquid	Alfa Aesar
40	Tetramethylbenzidine (TMB)	$C_{16}H_{20}N_2$	Solid	Merck
41	Glycine (Gly)	$C_2H_5NO_2$	Solid	Loba- Chem
42	Alanine (Ala)	$C_3H_7NO_2$	Solid	Loba- Chem
43	Valine (Val)	$C_5H_{11}NO_2$	Solid	Loba- Chem
44	Proline (Pro)	$C_5H_9NO_2$	Solid	Loba- Chem
45	Leucine (Leu)	$C_6H_{13}NO_2$	Solid	Loba- Chem
46	Lysin (Lys)	$C_6H_{14}N_2O_2$	Solid	Loba- Chem
46	Isoleucine (Ile)	$C_6H_{13}NO_2$	Solid	Loba- Chem
47	Serine (Ser)	$C_3H_7NO_3$	Solid	Loba- Chem
48	Threonine (Thr)	$C_4H_9NO_3$	Solid	Loba- Chem
49	Glutathione (GSH)	$C_{10}H_{17}N_3O_6S$	Solid	Loba- Chem
50	Phenylalanine (Phe)	$C_9H_{11}NO_2$	Solid	Loba- Chem
51	Trptophan (Trp)	$C_{11}H_{12}N_2O_2$	Solid	Loba- Chem
52	Tyrosin (Tyr)	$C_9H_{11}NO_3$	Solid	Loba- Chem
53	Methionine (Met)	$C_5H_{11}NO_2S$	Solid	Loba- Chem
54	Cysteine (Cys)	$C_3H_7NO_2S$	Solid	Loba- Chem
55	Glutamic acid (Glu)	$C_5H_9NO_4$	Solid	Loba- Chem
56	Glutamine (Gln)	$C_5H_{10}N_2O_3$	Solid	Loba- Chem
57	Aspartic acid (asp)	$C_4H_7NO_4$	Solid	Loba- Chem
58	Asparagine (asn)	$C_4H_8N_2O_3$	Solid	Loba- Chem
59	Arginine (arg)	$C_6H_{14}N_4O_2$	Solid	Loba- Chem

2.2.1 Bacterial strains

The antibacterial experiments were performed using two bacterial strains. *Escherichia coli* (*E. coli*) MTCC 739 (ATCC 10536) was originally procured from the Institute of Microbial Technology (Chandigarh, India). The *Staphylococcus aureus* (*S. aureus*) NCIM

5021 (ATCC 25923) strain was obtained from the National Chemical Laboratory (Pune, India). L.B. media (Himedia Lab. Ltd., Mumbai) was used for evaluating bacterial growth in liquid broth culture and was supplemented with a 2% bacteriological agar (Himedia Lab. Ltd., Mumbai) to prepare the solid media used in plate culture studies.

2.2.2 Cleaning solution

For the preparation of cleaning solution, 60 g of Potassium dichromate was dissolved in warm water, and cooled at room temperature. Thereafter, 60 mL concentrated H_2SO_4 was added slowly. Thus prepared cleaning solution was mixed thoroughly and used for cleaning purpose.

2.2.3 Sterilization

The dried glassware and media used for the antibacterial activity were sterilized in an autoclave for 20 min at 15 psi pressure at 121 ºC.

2.3 Methods

2.3.1 Preparation of leaf extracts

For the preparation of the aqueous leaf extract, the fresh leaves of *X. strumarium* and *C. bonplandianum* were collected from the institute campus (Indian Institute of Technology, Banaras Hindu University, Varanasi, U.P., Indian, 221005) and brought into the laboratory. Thereafter, the leaves were washed several times under tap water and then with UPW to remove dust and other adhering impurities. After that, the leaves were air dried under shade to eradicate the moisture completely. The dried leaves were then chopped into fine pieces and 25g of leaves were heated for 10 min in 100 mL of UPW. Finally, the aqueous extract of *X. strumarium* (AEX) and *C. bonplandianum* (AEC) were collected and filtered through

Whatman filter paper No. 1. The prepared AEX and AEC were stored as stock solution at 4°C and used within 3 days.

2.3.2 Confirmation and quantification of polyphenolic compounds

2.3.2.1 Ferric chloride test

The presence of polyphenolic compound was confirmed by performing Ferric Chloride test. For this 0.1% $FeCl_3$ solution was added into the AEX and AEC which resulted into a sudden color change from light yellow to dark green color (Dutta and Ray 2014). This change in color confirmed the presence of polyphenolic compound as shown in the **Scheme 2.1** given below.

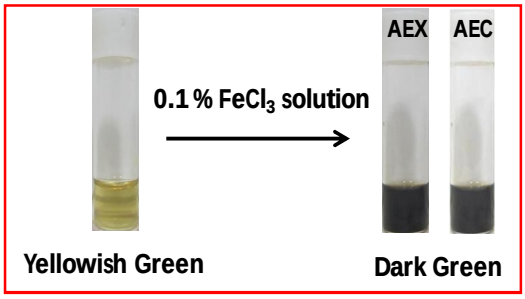

Scheme 2.1 Scheme showing the change in color from light yellow to dark green which confirmed the presence of polyphenolic in AEX and AEC

2.3.2.2 Folin Ciocalteu's method

Total phenolics content was estimated by Folin Ciocalteu's method. For this, 1 mL of plant extracts (AEX and AEC) or standard solution of prepared gallic acid (GE) (100, 200, 400, 600, 800, 1000 µg/mL) was added in test. Thereafter, 1 mL of Folin Ciocalteu's reagent (1N) was added to the above reaction mixture and shaken. After 5 minutes, 1.0 mL of 7 % Na_2CO_3 was added to the mixture, shaken and the total volume was made up to 10 mL with UPW. After 90 min, the absorbance was determined against reagent blank at 650 nm using

UV visible spectrophotometer (Ainsworth and Gillespie 2007). The experiments were performed in triplicates. The total phenolics content was expressed as µg Gallic acid Equivalents (GAE). The result showed that AEX and AEC were the rich source of phenolics having 4212 µg GAE/g and 2890 µg GAE/g respectively **(Fig. 2.1)**.

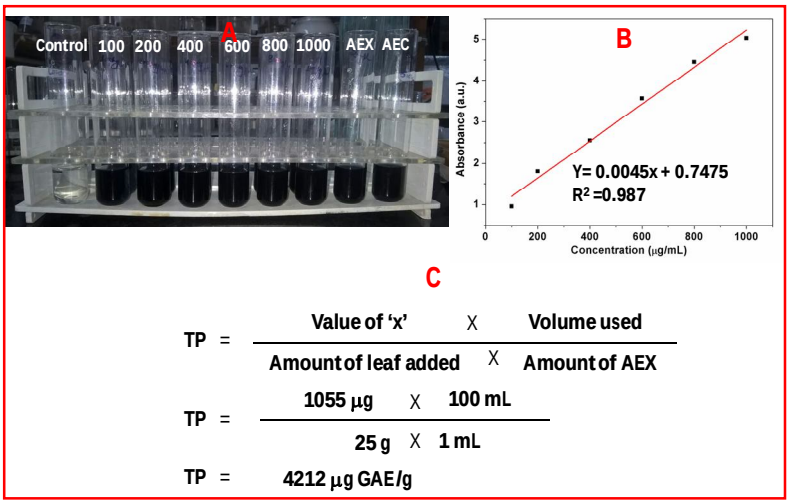

Figure 2.1 (A) Change in color of the reaction mixtures including control, different standard solution of GA, and AEX & AEC, (B) calibration curve of standard solutions of GA and, (C) calculation of total phenolics (TP)

2.3.3 Preparation of standards

All the standards were prepared in the UPW and the prepared standard stock solutions were stored at 4°C.

2.3.3.1 Preparation of standard solution of silver metal ion

The standard stock solution of silver metal ion was prepared using $AgNO_3$ as a precursor of silver. For this purpose, 0.170 mg of accurately weighed $AgNO_3$ was dissolved in the 100 mL of UPW in 250 mL Erlenmeyer flask covered with black paper. This standard solution was used as 10 mM stock solution of silver metal ion.

2.3.3.2 Preparation of standard solution of gold metal ion

The standard stock solution of gold metal ion was prepared using $HAuCl_4.xH_2O$ as a precursor of gold. For this purpose, 0.339 mg of accurately weighed $HAuCl_4.xH_2O$ was dissolved in the 100 mL of UPW in 250 mL Erlenmeyer flask covered with black paper. This standard solution was used as 10 mM stock solution of gold metal ion.

2.3.4 Green synthesis of AgNPs and AuNPs

2.3.4.1 Synthesis of AgNPs

Initially, the synthesis experiments of AgNPs using AEX and AEC were conducted with two sets of reaction mixtures each having 100 mL of 1 mM $AgNO_3$ solution using 2% AEX and 2.5% AEC inoculums dose (v/v). The $AgNO_3$ concentration and inoculum dose were selected arbitrarily. The first sets of reaction mixture were exposed to bright sunlight between 12 am and 2 pm for avoiding the fluctuations in solar intensity while other sets were kept in a black colored sealed vessel at dark conditions. The temperature of the ambient environment in bright sunlight and solar intensity while AgNPs synthesis were 38°C and 53600 lux respectively using AEX and 38°C and 53000 lux respectively using AEC. Whereas, the temperature of the dark condition and solar intensities were 28°C and 0 lux respectively in case of AEX and 30°C and 0 lux in case of AEC. The pH of the reaction mixtures was neutral. The first sets of reaction mixtures of AEX and AEC exposed to bright sunlight showed an instant color change from greenish yellow to reddish brown within few seconds whereas the reaction mixture of AEX and AEC kept at dark condition exhibited only a slight change in color up to 15 hrs and 24 hrs respectively which indicated the photocatalytic action of sunlight on the synthesis of AgNPs. Therefore, further all the AgNPs synthesis experiments were conducted in bright sunlight in order to optimize the process

variables using one factor at a time approach. The process variables used for the optimization purpose were duration of sunlight exposure, AEX and AEC inoculums doses and $AgNO_3$ concentration. After the optimization of these process variables, the synthesized AgNPs were purified. For purification purpose, thus obtained AgNPs from AEX and AEC were centrifuged at 15000 rpm for 15 min and subsequently re-dispersed in UPW to eliminate the uncoordinated biological molecules. This process was repeated four times and after drying the final mass of AgNPs was collected.

2.3.4.2 Synthesis of AuNPs

The synthesis of the AuNPs using AEX and AEC was performed following the similar route adopted for the synthesis of AgNPs. For the synthesis purpose, 3% (v/v) of AEX and 2% (v/v) of AEC inoculum doses were added into 2 mL of 0.8 mM $HAuCl_4.xH_2O$ and exposed to the sunlight. In order to investigate the effectiveness of photocatalytic activity of sunlight, the biosynthesis reactions of AuNPs were carried out both in ambient sunlight and dark condition. The temperature of the ambient environment in sunlight and solar intensity of incident sunlight radiation were 40 °C and 68600 lux respectively while synthesizing AuNPs using AEX whereas these were 39 °C and 66300 lux while synthesizing AuNPs using AEC. The temperature of the dark condition and light intensity were 34°C and 0 lux respectively in both the cases of using AEX and AEC. To avoid the fluctuation in temperature and sunlight intensity, the synthesis reactions were carried out between 12 pm to 2 pm. The reaction mixtures kept in sunlight exhibited the development of dark purple color and a sharp SPR band within 15 min and 16 min using AEX and AEC respectively. However the reaction mixtures of AEX and AEC keeping in dark failed to attain the same extent of color change even after 15 hrs and 10 hrs respectively. Therefore, further all the

AuNPs synthesis experiments were performed in bright sunlight for the optimization of the other process parameters using one factor at a time approach. The process parameters such as sunlight exposure time, AEX and AEC inoculums doses and $HAuCl_4.xH_2O$ concentration were optimized. After the optimization process, the synthesized AuNPs were purified by centrifuging at 15000 rpm for 15 min and subsequently re-dispersing in UPW to remove the water soluble molecules and other secondary metabolites. The final mass of AuNPs was collected by vacuum drying after repeating this process four times.

2.3.5 Synthesis of graphene oxide (GO) and reduced graphene oxide (rGO)

In this work, the GO was prepared according to our previously reported works (Singh *et al*. 2016, Mohan *et al*. 2016). For this, 3g graphite powder was added into the mixture of concentrated H_2SO_4/H_3PO_4 (360:40 mL). Thereafter, 15 g of $KMnO_4$ was added slowly into the above reaction mixture. After that the final reaction mixture was continuously stirred at 50° C for 12 hrs which was followed by the cooling at room temperature. The cooled reaction mixture was poured into 1 L of UPW by keeping it on the ice bath. Further, 3 mL of H_2O_2 (30%) was added with continuously stirring for additional 2 hrs. After that, the reaction product was centrifuged at 10000 rpm for 15 min. Further, the obtained material was collected and followed by several times washing with 5% HCl and then many times with UPW. Then final washed solid material i.e. GO was placed in the vacuum oven at 70° C for 24 hrs. The preparation of GO was followed by the preparation of rGO and for this, the GO thus obtained was suspended in UPW (1 mg/mL) and well dispersed using ultrasonication for 1 hr and then centrifuged at 10000 rpm for 10 min to avoid the unexfoliated GO. The centrifugation yielded brown colored suspension of GO which was decanted and reduced

hydrothermally using Ammonia solution (NH_3) and Hydrazine (NH_2NH_2). Briefly, the ammonia was used to maintain the pH of the solution up to 10 which was followed by the addition of N_2H_4 and stirred for 10 min. Further, the suspension was transferred to an autoclave (Teflon-lined) and kept at 200 ºC for 5 hrs. The final black colored suspension thus obtained was collected by centrifuging at 10000 rpm for 15 min several times with UPW.

2.3.6 Fabrication of AgNPs-rGO-PANI nanocomposite

For the synthesis of AgNPs-rGO-PANI nanocomposite, firstly, the rGO-PANI nanocomposite was prepared by using 1:100 mass ratio of rGO to aniline where 1.0 mg rGO and 100.0 mg aniline were added into 20 mL of HCl (2.0 mol/L) solution and sonicated for 30 min. Thereafter, 10 mL aqueous APS solution (0.04 g/mL) was added slowly into the above mentioned solution. After this, the solution was stirred for 5 hrs wherein it turned to dark green which indicated the synthesis of the rGO-PANI nanocomposite. After stirring, the rGO/PANI nanocomposite thus obtained was centrifuged at 10000 rpm for 15 min and washed with UPW. The above process was repeated four times for the removal of uncoordinated impurities and thereafter dried at 60ºC.

Thus obtained rGO-PANI nanocomposite was further used for the synthesis of AgNPs-rGO-PANI nanocomposite by a self-assembly method. For this, 0.01 g rGO-PANI nanocomposite was added into the 25 mL colloidal AgNPs synthesized from AEC and stirred for 10 hrs. After this, the final AgNPs-rGO-PANI nanocomposite was centrifuged at 10000 rpm for 15 min and washed several times with UPW and dried at 60 ºC.

2.3.7 Fabrication of AgNPs-rGO-PANI modified glassy carbon electrode

For the preparation of AgNPs-rGO-PANI modified glassy carbon electrode (AgNPs-rGO-PANI-GCE), ethanol-water (2:1) suspension AgNPs-rGO-PANI was deposited on GCE. After drying at room temperature, 15 µL of 1% Nafion solution was drop casted over the AgNPs-rGO-PANI-GCE, to enhance the adherence. The loading of electrochemical sensor mass (AgNPs-rGO-PANI) was maintained by 0.5 mg cm^{-2} on GCE. The GCE was found to be possessed 0.2 cm^2 active surface (Srirapu *et al*. 2014). Thus prepared AgNPs-rGO-PANI-GCE was used for the sensitive detection of H_2O_2.

2.3.8 Fabrication of AuNPs-rGO nanocomposite

The optimized AuNPs at several parameters synthesized from AEC was stable, smaller, and larger in number as compared to AuNPs obtained from AEX. Therefore, AEC synthesized AuNPs was used for the preparation of AuNPs-rGO nanocomposite. For this purpose, 2 mL of AuNPs suspension was added into 20 mL of 0.25 mg/mL rGO and stirred for 5 hrs. Thereafter, the final AuNPs-rGO nanocomposite was centrifuged at 10000 rpm for 15 min and washed four times with UPW and dried at 60 ºC for further characterization purpose.

2.4 Characterization

The synthesized AgNPs, AuNPs and the nanocomposites; AgNPs-rGO-PANI and AuNPs-rGO were characterized through several modern characterizing techniques. The following characterizing techniques are discussed here in brief.

2.4.1 UV-visible spectroscopy

UV-Visible spectroscopy is the study of interaction of light with the chemical compounds. When a beam of light passes through a chemical compound, it results in absorption, transmission and reflection of light over a certain range of wavelength. Spectrophotometry is used to measure the amount of light absorbed or transmitted by the chemical compounds. The transmittance is the ratio of the intensity of the light entering the sample (I_0) to that exiting the sample (I_t) at a particular wavelength and expressed as percentage transmittance (%T) (**Equation 2.1**).

$$\%T = \left(\frac{I_t}{I_0}\right) \times 100 \qquad 2.1$$

The negative logarithm of the transmittance is the absorbance (A) (**Equation 2.2**).

$$A = -\log T \qquad 2.2$$

The UV-visible range of the electromagnetic radiation ranges from 190-700 nm. Lambert's and Beer's laws are most important principles in absorption analysis. Lambert's law states that the fraction of radiation absorbed is independent of the intensity of the radiation and Beer's law states that absorption is proportional to the concentration of absorbing molecules. Combining these two laws, we can derive the Beer-Lambert's Law (**Equation 2.3)**.

$$\log_{10}\left(\frac{I_0}{I_t}\right) = \varepsilon c l \qquad 2.3$$

Where 'I_0' is the intensity of the incident radiation and 'I_t' is the intensity of the transmitted radiation. 'ε' is the molar absorption coefficient which is constant for each absorbing material, and having the units mol^{-1} dm^3 cm^{-1}, 'l' is the path of the length in cm, 'c' is the concentration of the absorbing molecule in mol dm^{-3}. non-bonding orbitals (lone pair electrons)

from lower to higher energy levels. The non-bonding orbitals are higher in energy comparatively π bonding orbitals which in turn are higher in energy than σ bonding orbitals. When the electromagnetic radiation of the correct frequency is absorbed, a transition occurs from one of these orbitals to an empty orbital, i.e. σ* or π*. The differences of energy among the orbitals depend on the bonding system and atoms present. Most of the transitions from bonding orbitals are of too short a wavelength (too high a frequency) to measure easily.

Therefore, most of the absorptions observed involve only π→π*, n→σ* and n→π* transitions. A common exception to this is the d→d transition of d-block element complexes (**Fig. 2.2**). In general, the UV-visible spectrometer consist two light sources, a monochromator, and a detector. Generally, the light sources are deuterium lamp and tungsten lamp which emit electromagnetic radiation in UV region and in the visible region of spectrum respectively.

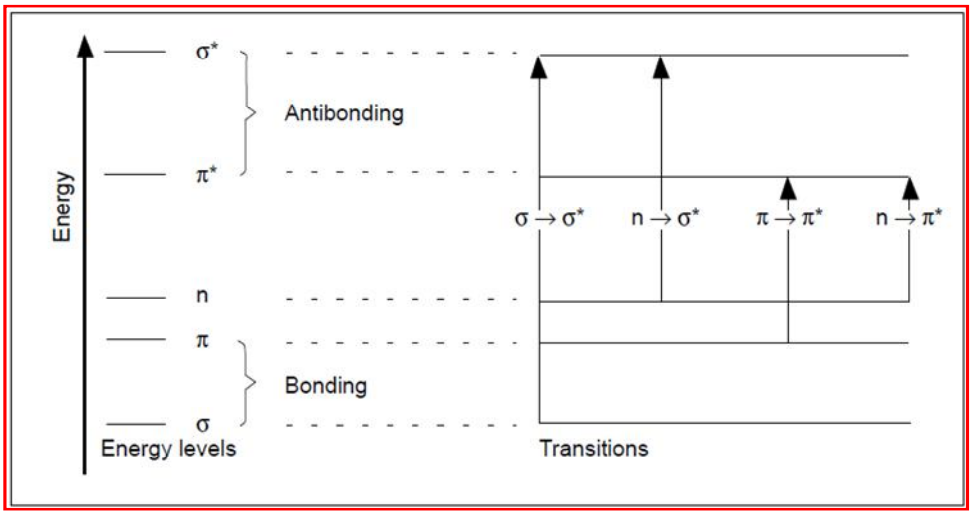

Figure 2.2 Possible electronic transitions in UV-visible spectroscopy

The important role played by the monochromator is the spreading of the beam of light into its component wavelengths. The detector is generally a photomultiplier tube (photodiodes in modern instruments) (**Fig. 2.3**).

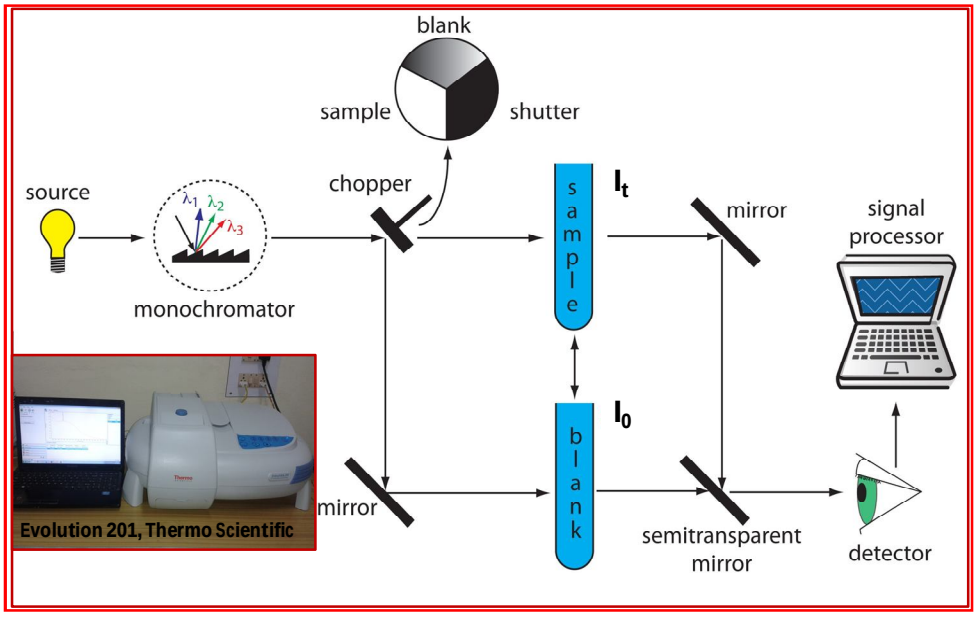

Figure 2.3 Schematic diagram of UV-visible spectrophotometer

In the current study, the UV-visible spectra were recorded using UV Visible spectrophotometer (Evolution 201, Thermo Scientific) in the range of 300 to 800 nm. The absorption of visible and ultraviolet radiation depends on the excitation of valence electrons present in single, or σ, bonding orbitals, and double or triple bonds (π bonding orbitals).

2.4.2 Fourier transform infrared spectroscopy

The involvement of various functional groups and their interaction among them was studied by Fourier transform infrared (FT-IR) spectroscopy. FT-IR spectroscopy is used to measure the vibrational mode of functional groups present in the sample. It can effectively identify the presence of different functional groups present in molecules or compounds. In FTIR spectroscopy, there are two mirrors, a movable (0 to 1 cm) mirror M1, and a fixed mirror M2 which receives a part of beam. The mirror M1, and M2 reflected back the rays along the same path and interacted with beam splitter (BS). Thereafter, the combined beam

falls on the sample and detector. The path length of the rays can affect the constructive and destructive interference occurring at BS. The recombined beam passing through the sample produces an absorption spectrum in which certain characteristic frequencies are absorbed by molecules present in the sample. Detector collects signal from sample in every millisecond and stores each spectrum in different locations (**Fig. 2.4**).

In the current study the FT-IR spectra were recorded using with the Perkin Elmer Spectrum 100 spectrophotometer. The instrument was equipped with the mid-infrared (MIR) radiation source which passed through the KBr window. The transmittance mode was preferred to obtain the spectra which were collected by the $LiTaO_3$ detector.

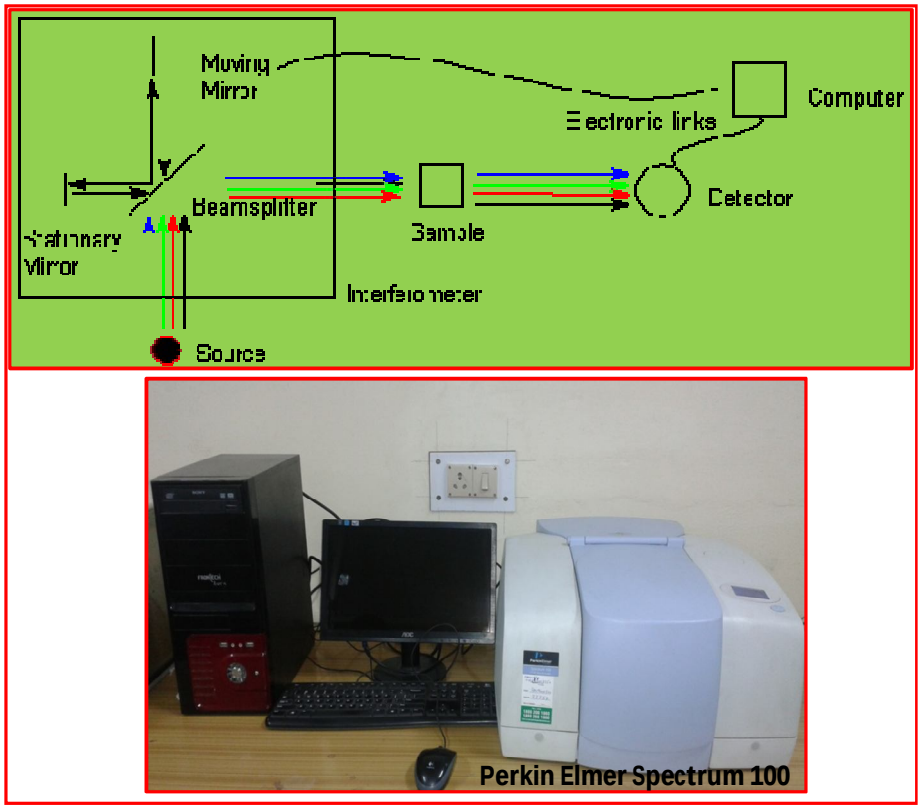

Figure 2.4 Schematic representation of working of Fourier transform infrared (FTIR) spectrophotometer and its photograph

The pellets of different samples were prepared by mixing with KBr in the approximate ratio of 1:100. Then the sample pellets were scanned within the range of 400-4000 cm^{-1} wavenumber with the spectral resolution of 4.0 cm^{-1} and scan speed 0.2 cm/sec.

2.4.3 X-Ray diffraction

The discovery of X-rays in 1895 by Rontgen and, diffraction of X-rays from a crystal by Laue Bragg in 1912 were the two very important events in the history of X-ray diffraction. Bragg's Law states that the interaction of cones of X-rays is related to interplanar spacing in the crystalline powder (West, 2007) (**equation 2.4**).

$$n\lambda = 2dsin\theta \qquad 2.4$$

Where, n is an integer, λ represents the wavelength of X-rays, d is interplanar spacing generating the diffraction, and θ is the diffraction angle. λ and d are measured in angstroms (́). The diffraction pattern of X-rays after interacting with the crystal plane is represented in **Figure 2.5.** The diffraction peaks of powdered samples having infinite amount of randomly oriented crystallites are measured along the 2θ. XRD consist three basic elements which are (i) an X-ray tube, (ii) a sample holder, and (iii) X-ray detector (**Fig. 2.6**). The cathode ray tube generates the X-rays by heating a filament to produce electrons which accelerated towards a target by applying a voltage and bombarding the target material with electrons. The X-ray spectra are produced when the electrons having sufficient energy dislodges the target material's inner shell electrons. These spectra consist of several components such as K_α and K_β. K_α consists of $K_{\alpha1}$ and $K_{\alpha2}$. $K_{\alpha1}$ has a slightly shorter wavelength and twice the intensity as $K_{\alpha2}$. The specific wavelengths are characteristic of target material (Cu, Fe, MO, Cr). The monochromatic X-rays needed for diffraction are produce by filtering through foils

or crystal monochromaters. Copper is most common target material for single-crystal diffraction with CuK_{α} radiation = 1.5418 Å.

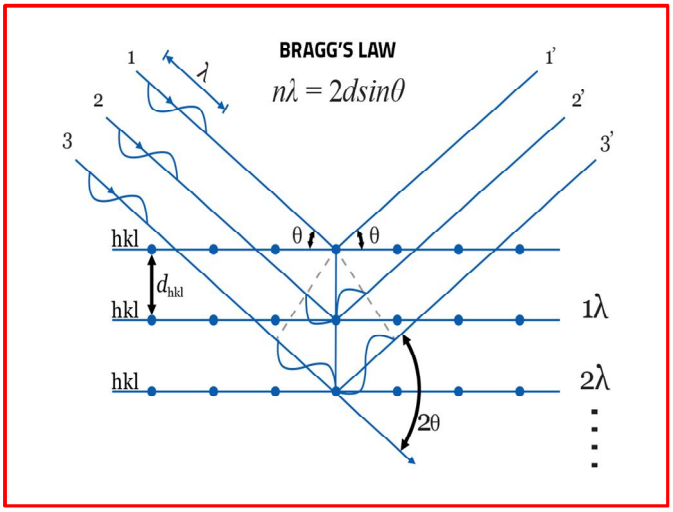

Figure 2.5 Illustration of X-rays diffraction by crystal plane

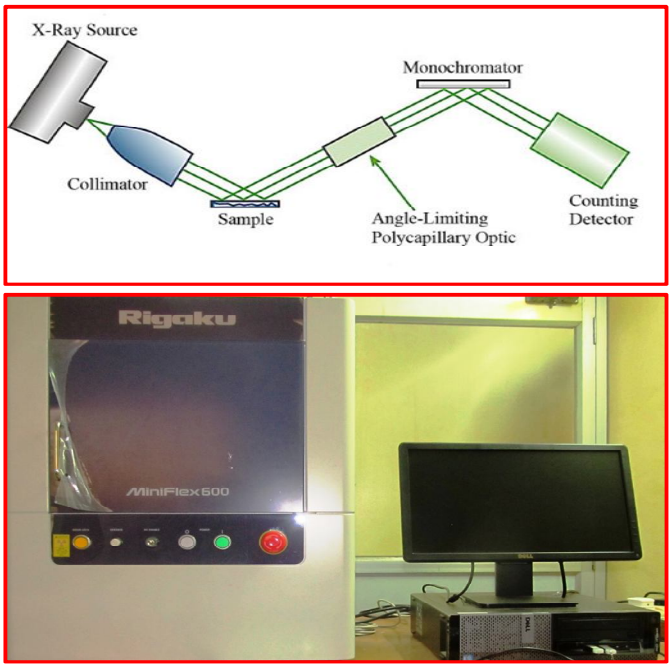

Figure 2.6 Representation of principle of powder X-ray diffraction and photograph of X-rays diffractometer

Thus generated X-rays are collimated and directed onto the sample. Thereafter, the intensity of the reflected X-rays is recorded with the rotation of the sample and detector. In the current study, the XRD of samples was obtained using MiniFlex600 (Rigaku, Tokyo, Japan). 40 kv voltage and 15 mA tube current was applied on the X-Ray tube for generating the Cu-Kα radiation (λ = 1.54059 Å). Thereafter, the X-Ray was allowed to pass through the graphite monochromater. The monochromatic X-Ray was targeted toward the sample by vertical goniometer having radius 150 nm with the accuracy of the ±0.02°. The diffracted X-Rays after the constructive interference were recorded by the NaI scintillator detector. The XRD patterns were recorded at scan rate of 2°/min with step size of 0.02.

2.4.4 Scanning electron microscopy

Scanning electron microscopy (SEM) is a powerful technique to determine the size, shape and elemental composition of the sample. It is a type of electron microscope with the aim of producing high resolution image. It was invented to avoid the limitation of the optical microscopy with increased magnification and higher resolution image. It is based on the interaction of incident electron beam and solid surface of the sample. The formation of the SEM image depends on the signals produced from the electron beam and specimen interactions. These interactions are of two types; elastic interactions and inelastic interactions. The elastic scattering is the outcome of deflection of the incident electron by the atomic nucleus or by outer shell electrons of similar energy of the specimen. The elastic scattering is characterized by negligible energy loss during the collision and by a wide angle directional change of the scattered electron. The backscattered electrons (BSE) are the incident electrons which elastically scatter through more than 90^{o} and yield a useful signal for imaging the sample.

Inelastic scattering is the outcome of several interactions between the incident electrons and the electrons of the sample. The amount of loss of energy depends on excitation of electrons either singly or collectively and on the binding energy of the electron. As a result, the secondary electrons (SE) are produced by the excitation of the electrons of specimen during the ionization of specimen atoms. The fundamental components of the SEM are shown in **Figure 2.7**. The topmost part of the SEM is electron gun which produces the electrons and accelerates them to an energy level of 0.1-30 keV. The diameter of electron beam produced by hairpin tungsten gun is too large to form a high resolution image.

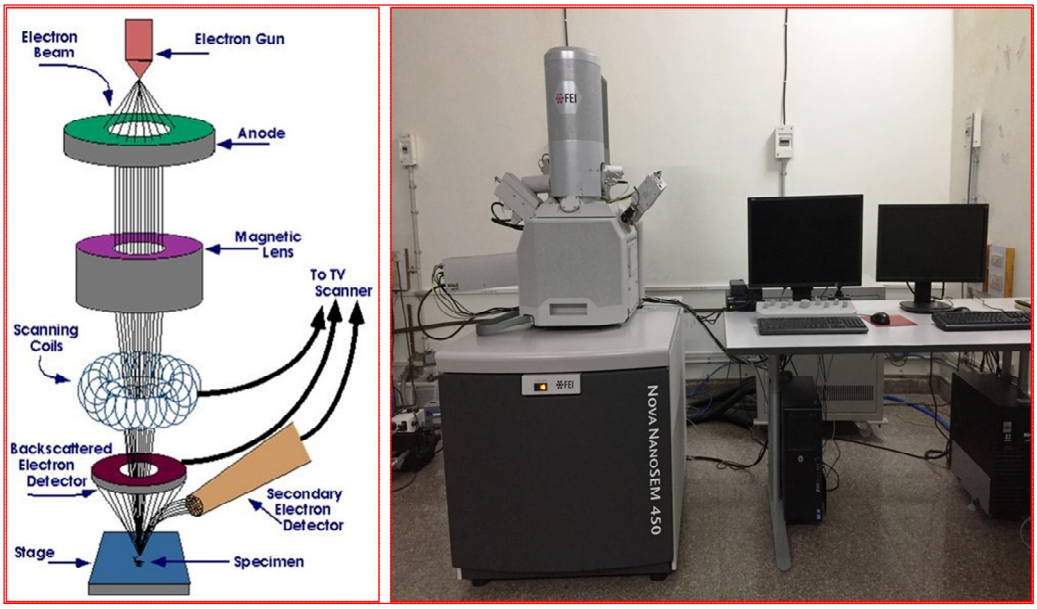

Figure 2.7 Representation of principle of Scanning electron microscopy and photograph of Scanning electron microscope

Therefore, for the purpose of focusing and defining the electron beam, and forming a small focused electron spot on the specimen, electromagnetic lenses and apertures are used. Due to this, the size of the electron source demagnetized down to the final required spot size (1-100 nm). A high vacuum environment, which allows the electrons to travel without

scattering by the air, is needed. The specimen stage, electron beam scanning coils, signal detection, and processing system provide real-time observation and image recording of the specimen surface.

In our current investigation, the SEM images of all the samples were obtained by using Field-Emission Scanning Electron Microscopy equipped with energy-dispersive X-ray analysis (SEM-EDX, Hitachi H-7100) at an accelerating voltage of 20 kV. The samples were loaded on the double sided carbon tape and further gold coated for obtaining the image.

2.4.5 Transmission electron microscopy

Transmission Electron Microscopy (TEM) is used to confirm the exact shape and size of the nanoparticles. It works on the basic principle of the light microscopy where the electron beam is used as a light source instead of utilizing light.

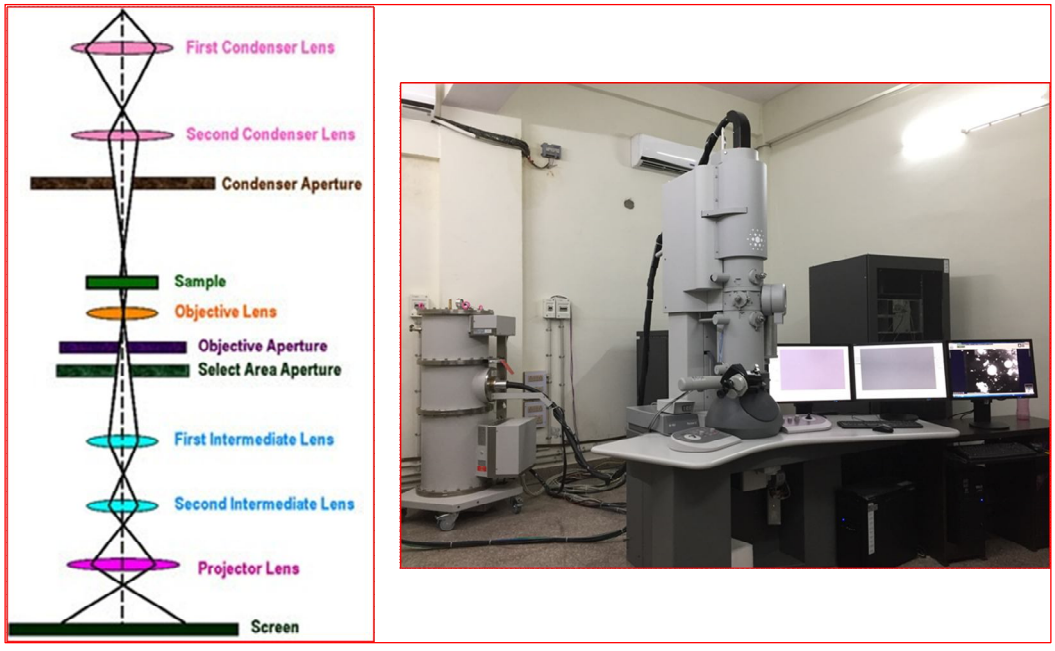

Figure 2.8 Representation of principle of Transmission electron microscopy and photograph of Transmission electron microscope

In a typical operational TEM, the voltage is used from 80-200 KV. In TEM, sample is imaged using by an electron beam with uniform electron density which is irradiated through the sample. Here the electrons are emitted by thermionic (lanthanum hexaboride or tungesten filament) or field emission (tungesten filament) electron gun. A set of condenser lenses control the illumination aperture and the area of the illuminated samples. The main function of the objective lense is to form image or diffraction pattern. In the current investigation both image and diffraction were determined (**Fig. 2.8**). The image provided the shape and size of the AgNPs and AuNPs whereas the diffraction pattern provided the crystalline nature. The distribution of electron density behind the specimen is magnified using a set of 3-4 stage lense system and viewed using fluorescent screen and the image is captured using CCD camera. At present, the TEM analysis has been significantly enhance after the integration of several advanced techniques into it such as energy dispersive X-ray (EDX) and electron energy loss spectroscopy (EELS).

In our current study, in order to investigate the shape, size, and diffraction pattern of the AgNPs and AuNPs, the TEM images were obtained using TECNAI 20 G2-Electron Microscope operated at accelerating voltage 200 kV. For this, the samples were prepared by simply dipping the copper film two times into the diluted samples and thereafter by drying it under the table lamp for 4 hrs. After that the samples were vacuum dried overnight and finally imaged.

2.4.6 Atomic force microscopy

Atomic force microscopy (AFM) belongs to a family of instruments called as scanning probe microscopes. It measures surface structure in length scale 10 nm-100 μm with high resolution and accuracy (lateral resolution~30 nm, vertical resolution~0.1 nm). The

principle of AFM functioning is completely different from scanning electron microscope, and provides a better analysis of nanoscale materials with minimal sample preparation (**Fig. 2.9**). It is based on a physical scanning of samples at sub-micron level using a probe tip of atomic scale and offers ultra-high resolution in particle size measurement. Depending upon properties, samples are usually scanned in contact or noncontact mode.

In contact mode, the cantilever/tip is allowed to be in contact with the surface of the sample in entire imaging process. The contact mode measures the surface topography of the sample by using a cantilever which is made of material having lower spring constant.

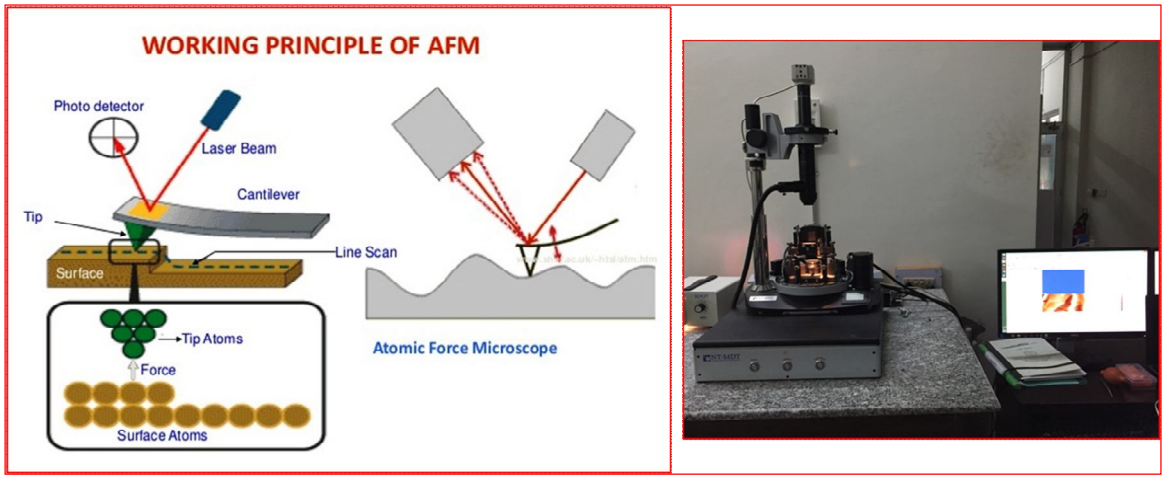

Figure 2.9 Representation of principle of Atomic force microscopy and photograph of Atomic force microscope

As the cantilever remains at the surface, the tip gets deflected by changing the height of surface features. The height of the tip can be adjusted using the feedback system of AFM to follow the contour and to maintain a constant tip pressure at the surface. The use of low spring constant materials and the feedback serves to preserve the integrity of the tip while imaging the sample. During the imaging, an abrupt change in surface feature height may

occur due to the incapability of the system to handle, and damaging and destroying the tip. The AFM requires the samples should be mounted on a very flat surface because the height limitation of many AFMs is only in the 10-15 μm range. To avoid the damaging of the sample, tapping or intermittent contact mode imaging is preferred. In this mode, the cantilever is driven by a piezoelectric resonator in a frequency range of 150 – 300 KHz. In this mode cantilever used is made up of higher spring constant material which provide higher resonant frequency to the cantilever/tip and the overall system.

One of the prime advantages of AFM is its ability to image non-conducting samples without any specific treatment. This feature allows the imaging of delicate biological and polymeric nano and microstructures. Moreover AFM (without any mathematical calculation) provides the most accurate description of size, size distribution and real picture which helps in understanding the effect of various biological conditions.

2.4.7 Zeta potential

The electric potential at the boundary of the double layer is known as the Zeta potential of the particles and has values that typically range from +100 mV to -100 mV. It is represented by the Greek letter zeta (ζ), hence called ζ – potential. The ζ – potential measures the magnitude of the electrostatic or charge repulsion/attraction between particles. It is one of the fundamental parameters which affect the stability of the particles. The measurement of ζ – potential explains the reason behind the dispersion, aggregation or flocculation. Therefore, it can be used to improve the formulation of dispersions, emulsions and suspensions. The pH of the sample is one of the most important factors which affect the ζ – potential.

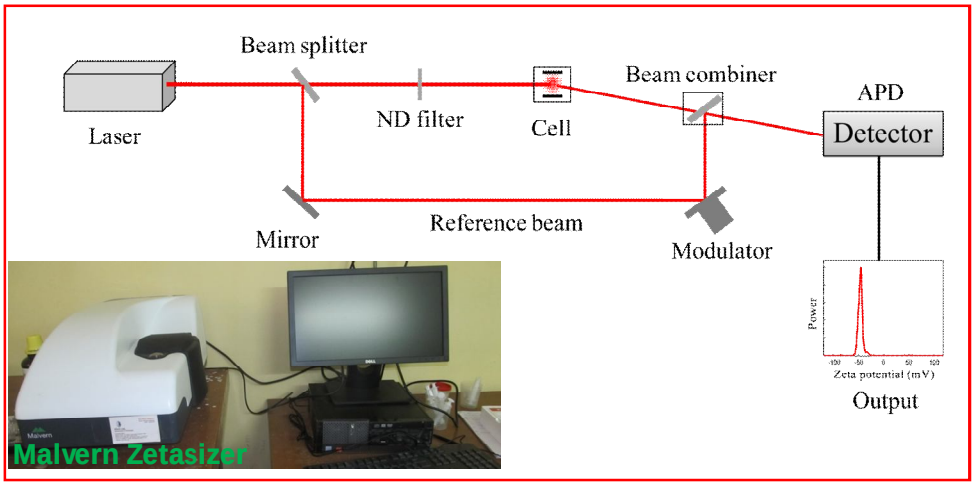

Figure 2.10 Working principle of Zeta potential and photograph of Zetasizer

It is positive at low pH and negative at high pH. The working principle and the digital image of the zetasizer are given in **Figure 2.10.** In the current investigation, the ζ – potential was measured using Malvern Zetasizer (Malvern Instruments, Ltd.).

2.5 Environmental and biological applications

2.5.1 Antibacterial study

2.5.1.1 Determination of minimum inhibitory concentrations of AgNPs

The optimized AgNPs obtained from AEX and AEC were investigated for antibacterial activity against both Gram-positive (*S. aureus*) and Gram-negative (*E. coli*) bacteria. For this firstly, the minimum inhibitory concentrations (MICs) of AgNPs was determined using bacterial strains grown in MHB. To determine the MIC, the standard populations of the cell suspensions were obtained by measuring the turbidity with a spectrophotometer. The synthesized AgNPs from AEX and AEC were twofold micro diluted in a standard broth to perform the susceptibility tests. The MHB grown bacterial strains of

mid-log phase (1×10^6 cells/mL) were diluted in fresh MHB. Thereafter, 0.1 mL of the diluted cell suspension was dispensed into each well of a 96-well microtiter plate. After that, the cells of *E. coli* and *S. aureus* were exposed to different concentrations of AgNPs (w/v) synthesized from AEX and AEC and the growth was regularly monitored at 600 nm using a microplate reader.

The MICs were considered as the lowest concentrations of the AgNPs inhibiting the visible growth of the bacteria. The AgNPs concentration that reduced the number of susceptible cells by less than 20% after 24 hrs of incubation was considered as MIC.

2.5.1.2 Disc diffusion assay

The antibacterial activity of the AgNPs synthesized from AEX and AEC was also evaluated by the disc diffusion method (Watts *et al*. 2008). For this purpose, the *S. aureus* and *E. coli* cells were grown in MHB at room temperature at 150 rpm. Thereafter, the bacterial pathogens (10^6 CFU/mL) were spread plated over the MHA plates. These inoculates were applied to the MHA plates along with control discs. The similar experiments were carried out with AgNPs and delivered on 6 mm sterile discs. Firstly, the plates were pre-incubated at 4 ºC for half an hour for the uniform diffusion. Further, the plates were incubated at 37 ºC for 24 hrs. After the incubation at 37 ºC for 24 hrs, the zones of inhibitions were determined by subtracting the disc diameter from the diameter of the total inhibition zone.

2.5.1.3 Cell viability test

The overnight grown cells of *E. coli* and *S. aureus* in MH broth at 37 ºC were used for the cell viability test. These cells were re-grown in fresh medium for 4 hrs before being

collected by centrifugation and further suspended in saline solution. For this purpose, the cell suspensions containing 10^6 cells/mL were incubated with 1.68 µg/mL AgNPs for *E. coli* and 2.55 µg/mL AgNPs for *S. aureus* synthesized from AEX. Similarly, the cell viability study of AgNPs synthesized from AEC was also investigated by adding 0.53 µg/mL AgNPs against *E. coli* and 0.64 µg/mL AgNPs against *S. aureus* at 37 ºC without shaking. The colony counting method was preferred for evaluating the loss of cell viability of *E. coli* and *S. aureus* where 100 µL solution of both the cells were spread onto LB plates separately and grown overnight at 37 ºC. The degree of inhibition in cell growth was determined after counting the colonies and comparing with the control plates. The isotonic saline solution devoid of AgNPs was used as a control. All the tests were performed in triplicates and the average results were reported.

2.5.1.4 Evaluation of antibacterial mechanism of AgNPs

The antibacterial mechanism of AgNPs synthesized from both AEX and AEC was determined by using a modified *o*-nitrophenol-β-D-galactopyranoside (ONPG) method where the measurement of activity of β-D-galactosidase was taken in to account (Gao *et al.* 2006, Chen *et al*. 2012). Briefly, a standard solution containing a cell suspension of 1 mL (10^6 CFU mL^{-1}) and 1 mL of ONPG solution (25 mM) were added simultaneously into 5.5 mL PBS (pH 7.4) and further incubated at 37 ºC for 15 min with shaking. Firstly, 100 µL of AgNPs (1.68 µg/mL and 0.53 µg/mL synthesized from AEX and AEC respectively, for Gram-negative bacteria) was added into a 96-well plate and labeled separately. Thereafter, 100 µL of the above standard solutions containing the cell suspensions and ONPG in PBS buffer were added in the respective wells and labeled. The changes of optical density at 420 nm were measured at different time interval using a Multi-label Microplate Reader (Perkin Elmer

VICTOR 3). The similar experiment was also performed for Gram-positive bacteria using 2.55 µg/mL and 0.64 µg/mL AgNPs as MIC synthesized from both AEX and AEC respectively.

2.5.1.5 Cell morphology observation

The bacterial cell morphology of the normal (without AgNPs) and effected cells (treated with AgNPs) were observed by incubating log phase *E. coli* and *S. aureus* cells at 37 ºC without shaking for 4 hrs. Thereafter, the collected cells were washed several times with PBS (pH 7.0). Further, the cells were fixed with glutaraldehyde solution for next 2 hrs. After that, the cells were sequentially dehydrated by treating with 50, 70, 80, 90, and 100% ethanol for the next 10 min. Consequently, the cells were gold sputter-coated and imaged using SEM.

2.5.2 Antileishmanial study

2.5.2.1 Parasites and culture conditions

L. donovani (BHU 1035) promastigotes were grown at 25°C and cultivated in M199 medium with L-Glutamine containing 15% fetal bovine serum. The cells were grown in 25T culture flasks with M199 medium with L-Glutamine containing 15% fetal bovine serum. *L. donovani* (BHU 1035) cells (3×10^5 cells / mL) were added to a flask containing 5 mL M199 medium with L-Glutamine containing 15% fetal bovine serum and 1M HEPES in a humidified atmosphere at 37°C and 5% CO_2. Cells were passaged when they reached 80-90% confluence.

2.5.2.2 *In vitro* Antileishmanial activity

The effects of different concentrations of AEX synthesized AgNPs (5, 2.5, 2, 1.5, 1.0 and 0.5 µg/mL) on the viability of the *L. donovani* were performed in 96-well flat-bottom

tissue culture plates. Logarithmically growing *L. donovani* promastigotes were harvested and counted using a Neubauer chamber and their concentration was adjusted to 1×10^6 cells/mL in culture medium. The promastigotes were plated in 200 µL aliquots (2×10^5/ well) and were cultured with AEX synthesized AgNPs. After 48 hrs of incubation at 25 °C the number of viable parasites were determined using 3-(4, 5-dimethylthiazol-2-yl)-2, 5-diphenyl-tetrazolium bromide (MTT) assay. After incubation, 10 µL of MTT solution (10 mg/mL) was added to all of the wells and the microplates were then incubated at 25 °C for 4 hrs. Generation of formazan crystals was observed microscopically while cell viability values were determined quantitatively using a microplate reader at 570 nm.

2.5.2.3 *In vitro* assay of cytotoxicity on J774A.1 macrophages

For this the J774A.1 cell line was incubated in a 96-well plate containing 2.5×10^4 cells/well. The plates were incubated overnight in a CO_2 incubator with a supply of 5% CO_2 at 37 °C for 24 hrs for adhesion of macrophages to the bottom of the well. The non-adherent cells were removed by washing with the M199 medium. The test and reference drugs of AgNPs (10, 5, 2.5, 1.25, 0.6, 0.3, 0.16 and 0.08 µg/mL) were dispensed in triplicate and three wells were left as control wells. After 30 min the plates were incubated for 72 hrs and an MTT assay was performed to assess cell proliferation or viability. Briefly, 10 mL of MTT was added to all wells at concentration of 10 mg/mL and incubated for 4 hrs. Then 100 µL of dimethyl sulfoxide was added to each well and quantitative analysis was carried out by using a microplate reader for subsequent determination of the absorbance at 570 nm. The experiment was performed twice for reproducibility and the concentration required to kill 50% of the cells (CC_{50}) was calculated.

2.5.2.4 Giemsa staining

Parasite cultures (10–20 µL) that had been exposed to AgNPs in test tubes were spreaded on microscope slides. These slides were then fixed in methanol for 5 minutes. After fixation, Giemsa stain (Sigma, St Louis, MO) was applied to the slides for 45 minutes and then they were examined with an inverted microscope (magnification 100X) (Olympus CK40; Olympus, Japan).

2.5.3 *In vitro* antioxidant assays

2.5.3.1 DPPH free radical scavenging assay

To investigate the radical scavenging potential of the AEC synthesized AgNPs, 1,1-Diphenyl-2-picrylhydrazyl (DPPH), a stable free radical was used according to our previously used method (Kumar *et al*. 2016). For this different concentrations (10, 20, 30, 40, 50, 75 and 100 µg/mL) of AgNPs and standard ascorbic acid were taken in different test tubes. After this 1 mL of freshly prepared DPPH (1 mM) dissolved in methanol was added to the above samples and vortexed thoroughly. Thereafter, the solutions were incubated in a dark place for 30 min and absorbance was recorded at 517 nm. The DPPH (devoid of AgNPs) was used as a control to compare the scavenging activity of AgNPs using the same procedure. The free radical scavenging activity was expressed as the percentage of inhibition that was calculated using the equation of DPPH radical scavenging activity (%)

$$= (Ac - As) / Ac \times 100 \qquad 2.5$$

Where Ac is the control absorbance of DPPH radical + methanol; As is the sample absorbance of DPPH radical + sample AgNPs/standard Ascorbic acid.

2.5.3.2 Hydrogen peroxide scavenging assay

The H_2O_2 scavenging activity was assayed by slightly modified method as reported by Pick and Mizel (Pick and Mizel 1981). In brief, different concentrations (10, 20, 30, 40, 50, 75 and 100 µg/mL) of AEC synthesized AgNPs and ascorbic acid (control) were mixed with 50 µL of 5 mM H_2O_2 solution and incubated at room temperature for 20 min. After that, the absorbance was measured at 517 nm and the percentage of H_2O_2 scavenging was calculated using Eq. (2.5).

2.5.4. Colorimetric detection of iron (Fe^{3+})

The AgNPs synthesized from AEC was investigated against colorimetric detection of metal ions. For the colorimetric detection of Fe^{3+}, 2 mL of AgNPs solution was used as primary testing sample. Then 100 µL of individual metal ions such as Fe^{3+}, Fe^{2+}, Pb^{2+}, Cd^{2+}, Co^{2+}, Zn^{2+}, Ni^{2+}, Al^{3+}, As^{3+}, Cu^{2+}, Hg^{2+}, Mn^{2+} were added into AgNPs and change in SPR band intensity was monitored using UV–vis spectrophotometer. The maximum quenching in the emission spectra of AgNPs and disappearance of color was observed only in the presence of Fe^{3+}. Therefore, different volume ranges of Fe^{3+} (25 µL-225 µL) were used to determine the linear detectable range by means of quenching in AgNPs SPR spectra.

2.5.5 Electrochemical detection of H_2O_2

CV and amperometric response of AgNPs-rGO, AgNPs-rGO-PANI-GCE was performed in 0.1 M PBS solution containing 0.5 M KCl at pH 7. The amperometric response of AgNPs-rGO-PANI-GCE in PBS in the presence of H_2O_2 at pH 7 led to the appearance of the response current at -0.4 V. All the CV and amperometric response experiments related to the H_2O_2 detection were carried out in N_2-medium. The electrochemical impedance

spectroscopy (EIS) was performed by applying the frequency in the range of 0.01-105 Hz at open cell potential.

2.5.6 Peroxidase-like catalytic activity of green synthesized AuNPs

The peroxidase like activity of the green synthesized negatively charged AuNPs (NC-AuNPs) from AEX and AEC were investigated using NC-AuNPs+TMB+H_2O_2 system where TMB was taken as a peroxidase substrate which produced blue color and intense spectra at 652 nm in oxidized TMB (oxTMB). For this, 50 µL H_2O_2 (1 mM) and 50 µL TMB (1 mM) were added into 200 µL of 0.2 M NaAc buffer (pH 4). Thereafter, 50 µL of optimum synthesized NC-AuNPs obtained from AEX and AEC were added into the above reaction mixture and incubated for 60 min and 20 min respectively. The control experiments were performed in the absence of NC-AuNPs and H_2O_2 using same reaction system

2.5.6.1 Colorimetric detection of H_2O_2

The peroxidase like mimicking activity of the green synthesized AuNPs from AEX and AEC was investigated for the colorimetric detection of H_2O_2. For this, 50 µL of different concentrations of H_2O_2 were added into and 50 µL TMB (1 mM), 50 µL of optimum AuNPs from both AEX and AEC and 200 µL of NaAc buffer (pH 4) system.

2.5.6.2 Detection of glutathione

The colorimetric detection of the GSH was carried out by adding 50 µL TMB (1 mM), 50 µL H_2O_2 (1 mM) and 50 µL AuNPs into 200 µL of 0.2 M NaAc buffer (pH 4). After that the reaction mixture was incubated in dark for 10 min at room temperature (32 ºC) which was followed by adding different concentration of GSH and monitored through UV-vis spectrophotometer.

2.5.6.3 Detection of cholesterol

For this purpose, firstly, 100 µL of different concentrations of ChO in of 0.1 mM PBS (pH 7.0) were treated with 20 µL ChOx (1 mg/mL) and incubated in dark for 10 min at 37 ºC to produce H_2O_2. Thereafter, 50 µL TMB (1 mM) and 50 µL of AuNPs-rGO in 200 µL 0.2 M NaAc buffer (pH 4) were added to the above reaction mixture and incubated for next five min at the same temperature. After that, the corresponding absorbance was measured at 652 nm using UV-visible spectrophotometer and the digital images were taken.